Lithium Insertion in LiCr3O8, NaCr3O8, and KCr3O8 at Room Temperature and at 125°C

Koksbang, R.; Fauteux, D.; Norby, P.; Nielsen, K. A.

Published in:
Journal of The Electrochemical Society

Link to article, DOI:
10.1149/1.2096695

Publication date:
1989

Document Version
Publisher's PDF, also known as Version of record

Lithium Insertion in $LiCr_3O_8$, $NaCr_3O_8$, and KCr_3O_8 at Room Temperature and at 125°C

R. Koksbang* and **D. Fauteux*,[1]**

H&L Engineering, Vestergade 24, 5700 Svendborg, Denmark

P. Norby

Institute of Chemistry, University of Oslo, Blindern, Oslo 3, Norway

K. A. Nielsen

Institute of Mineralindustry, Technical University of Denmark, 2800 Lyngby, Denmark

ABSTRACT

Lithium insertion and deinsertion reactions have been carried out with $LiCr_3O_8$, $NaCr_3O_8$, and KCr_3O_8 chemically and electrochemically at room temperature and at 125°C. The electrochemical experiments were performed with a nonaqueous liquid electrolyte at room temperature and with a polymer electrolyte at high temperature. At both temperatures, $LiCr_3O_8$ inserts chemically and electrochemically *ca.* 4 and 5 Li per formula unit, respectively. Experimental data reveal that the reaction involves major structural changes. Insertion of only small amounts of Li leads to irreversible structural breakdown. At elevated temperatures, the isostructural compounds $NaCr_3O_8$ and KCr_3O_8 are able to accommodate more than $4Li/MCr_3O_8$. During this process, minor structural changes are observed. At room temperature, $NaCr_3O_8$ and KCr_3O_8 also accommodate Li topotactically, but the maximum number of Li inserted per formula is close to $4Li/NaCr_3O_8$ and 1.3 Li/KCr_3O_8. Lithium ion diffusion coefficients are similar for the two compounds in the comparable composition range. Thermally, the fully lithiated compounds appear to be as stable as the pristine materials.

In chromium-oxygen compounds, prepared by conventional high-temperature/pressure methods, chromium tends to be present as Cr(III), Cr(VI), or as a mixture of these two oxidation states. Attempts to prepare ternary chromium oxides containing other transition metals and chromium in intermediate oxidation states usually fails due to a self-redox reaction in which chromium is stabilized as Cr(III) and/or Cr(VI) while the transition metal is either oxidized or reduced, respectively. Similarly, attempts to prepare mixed-oxidation-state chromium oxides usually leads to dismutation, *e.g.*

$$3Cr(IV) \rightarrow 2Cr(III) + Cr(VI)$$

or

$$3Cr(V) \rightarrow Cr(III) + 2Cr(VI)$$

However, apart from CrO_2, tetravalent chromium occurs in, *e.g.*, $ACrO_3$, A_2CrO_4, and A_3CrO_5 compounds (A = group IIA metal) (1), while pentavalent chromium occurs in hypochromates, *e.g.*, as $Ba_3(CrO_4)_2$, Li_3CrO_4, and K_3CrO_4 (2, 3).

Insertion/deinsertion reactions of alkali metal ions in transition metal oxides often lead to unusual products impossible to prepare by conventional methods and are thus a possible route to chromium oxides containing chromium in intermediate or mixed oxidation states.

Lithium and sodium extraction has been investigated in the layered oxides $LiCrO_2$ and $NaCrO_2$ by both chemical and electrochemical methods (4). Partial change of the oxidation state from +3 to +4 is observed in both systems without structural changes. In materials research for lithium battery systems, various binary chromium oxides have been investigated (5-10). The main interest has focused on Cr_3O_8 and Cr_2O_5 due to the high specific energies observed for the Li/CrO_x couples, exceeding 1000 Wh/kg for Li/Cr_3O_8. These oxides apparently contain only Cr(III) and Cr(VI) (11), and lithium insertion presumably only involves reduction of Cr(VI) to lower oxidation states (5). Although the structures of Cr_2O_5 and Cr_3O_8 are still unknown, and the lithiated products are x-ray amorphous, it was suggested that the lithium insertion reaction is topotactic (5).

Contrary to Cr_3O_8 and Cr_2O_5, the structures of the three ternary chromium oxides $LiCr_3O_8$, $NaCr_3O_8$, and KCr_3O_8 are known. The structure of $LiCr_3O_8$ is shown in Fig. 1a and that of the two isostructural compounds $NaCr_3O_8$ and KCr_3O_8 are shown in Fig. 1b. The $LiCr_3O_8$ structure is composed of (Li, Cr)O_6 octahedra, which forms staggered strings by edge sharing in the direction of the c-axis, and CrO_4 tetrahedra which connects the octahedra strings to a three-dimensional framework by corner sharing. Each tetrahedron is in contact with three different strings. The lithium and chromium atoms are randomly distributed on the octahedral sites (12). Similarly, the (Na, K)-type is made of CrO_6 octahedra and CrO_4 tetrahedra that form layers by corner sharing. The layers are held together by the interlayer alkali metal atoms. The oxygen coordination number of sodium and potassium is 10 (13).

The close similarity of the two structures is obvious if the layers of the (Na, K)-type are packed closer together. In this way the coordination number of the Na or K is reduced to 6 as in $LiCr_3O_8$. The metal-oxygen arrangement is now the same in both structures when the random distribution of lithium and chromium in $LiCr_3O_8$ is not taken into consideration (14).

The observed octahedral and tetrahedral chromium-oxygen distances differ considerably and are in agreement with the chromium-oxygen distances expected from

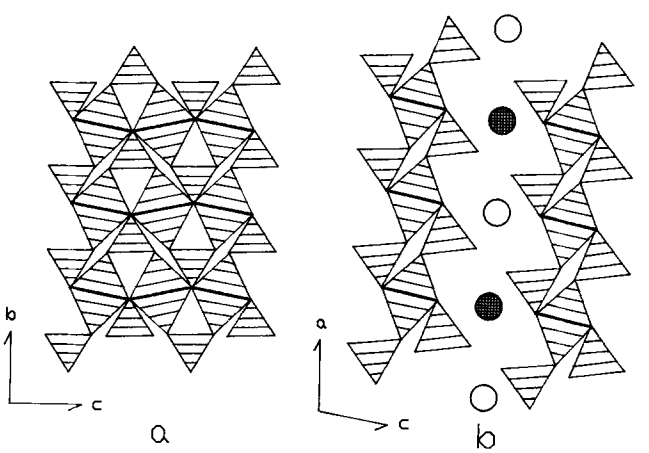

Fig. 1. $LiCr_3O_8$ (a) and (Na, K)Cr_3O_8 (b) structures shown as oxygen tetrahedra/octahedra representation projected on the (011) and (101) plane, respectively (12).

* Electrochemical Society Active Member.
[1] Present address: Mead Imaging, Miamisburg, Ohio 45342.

standard ionic radii for Cr(III) and Cr(VI), respectively (15). Measurements of the magnetic susceptibility (16) and x-ray photoelectron spectrum (17) of KCr_3O_8 support the crystallographic conclusion that chromium is essentially present as trivalent chromium (octahedra) and hexavalent chromium (tetrahedra) in the ratio 1:2.

The structure adopted by $NaCr_3O_8$ and KCr_3O_8 provides possible lithium diffusion paths in two dimensions between the $(Cr_3O_8^-)_n$ layers. Within the layers and parallel to them are one-dimensional channels of *ca.* 1Å diam, which are larger than the average interlayer spacing. In $LiCr_3O_8$, these channels are the only diffusion paths left in the structure. Eight four-coordinated sites per unit cell corresponding to four lithium atoms inserted per formula unit, can be identified inside the channels.

The observed oxygen coordination around chromium is tetrahedral for Cr(VI) and Cr(V), tetrahedral or octahedral for Cr(IV), and octahedral for Cr(III) (2). It should therefore be possible to reduce the tetrahedral Cr(VI) to Cr(IV) without major structural rearrangements, corresponding to four lithium per formula unit. Reduction of Cr(VI) to Cr(III) must lead to structural breakdown.

Except for a preliminary paper on lithium and sodium insertion in these oxides at elevated temperature (15), they seem to have been neglected so far. At temperatures above 100°C, all three compounds are able to accommodate more than four lithium atoms per formula unit corresponding to 850-1100 Wh/kg oxide.

In the present paper, the previous work has been extended to room temperature lithium insertion/deinsertion reactions, and a comparison is made with the results obtained at elevated temperature.

Experimental

The chromium oxides were prepared by heating 2:1 molar ratio mixtures of CrO_3 (Merck, p.a.) and $M_2Cr_2O_7$ (Merck, p.a.) placed in quartz crucibles to 350°C in open air for *ca.* 2h (18). Deviation from stoichiometry was induced by variation of the preparation conditions. In the following the compounds will be referred to as MCr_3O_8 irrespective of the actual compositions reported in Table I. Excess $M_2Cr_2O_7$ could be removed by washing with distilled water because the black MCr_3O_8 compounds are insoluble in water (18). X-ray diffraction diagrams of $NaCr_3O_8$ and KCr_3O_8 were in good agreement with the literature (13-14) and no other phases were observed. $LiCr_3O_8$ proved to be more difficult to obtain in the pure state. Additional lines compared to the published powder patterns (12, 14) were present in the x-ray diagram of the sample used for the room-temperature experiments. The identity of these impurities could not be fully established but are probably caused by binary chromium oxides formed by decomposition of CrO_3 (19). However, lithium insertion in CrO_x takes place at voltages above 3.0V (8), whereas the lithium insertion in $LiCr_3O_8$ takes place at lower voltage (Fig. 2a and 3a). The amount of CrO_x impurities present in the sample was therefore considered to be low. The x-ray patterns of $NaCr_3O_8$ and KCr_3O_8 were indexed on the basis of a monoclinic unit cell in the space group C2/m (14). Lattice parameters were refined using a least squares routine and are given in Table I with the chemical composition of the compounds.

For chemical lithium insertion/deinsertion reactions, the following solutions were used: 1.6*M* n-BuLi (Merck) in hexane, 0.6*M* LiI, I_2, and Br_2 (Merck, p.a.) in acetonitrile (21, 22). Typically, a known amount of solid oxide was dispersed in hexane or acetonitrile followed by slow addition of excess of one of the above-mentioned solutions. The suspensions were stirred for 2-3 weeks before filtering, repeated washing with acetonitrile, and vacuum drying at room temperature. The alkali metal and chromium content of the compounds were determined by flame photometry and atomic absorption.

X-ray diffraction analysis was conducted using Cr $K_{\alpha 1}$ (λ = 2.2897Å, Guinier-Hägg camera) radiation and Si as internal standard (a = 5.43088Å). DSC measurements were made using a Stanton Redcroft STA 785, and infrared spectra were recorded on a Perkin Elmer 883 spectrophotometer using either the potassium bromide tablet technique or nujol mulls. No differences were observed between the two types of spectra.

Polymer electrolyte films of 25-50 μm thickness were solvent cast on an insert substrate from an acetonitrile solution of PEO (M.W. $6 \cdot 10^5$, BDH) and $LiCF_3SO_3$ (Flourad FC 124, 3*M*) in the molar ratio 9:1 and dried overnight at 60°C in vacuum. Composite cathodes were solvent cast from acetonitrile solutions/suspensions on Ni foil and dried at 120°C in vacuum overnight. The compositions of the cathodes were 50-60 weight percent (w/o) MCr_3O_8, 10 w/o acetylene black, and 30-40 w/o $(PEO)_9LiCF_3SO_3$, and the thickness was *ca.* 50 μm. Cells were assembled by placing a cathode on one side of a piece of polymer electrolyte (50 μm thick) and a cleaned piece of lithium foil on the other side. The cells were mounted between spring-loaded Ni-plated brass disks and housed in sealed brass containers.

The liquid electrolyte used was 0.5*M* $LiCF_3SO_3$ in propylene carbonate, vacuum distilled over sodium, and further dried with freshly cut lithium pieces. The cathodes were made by mixing 50 w/o MCr_3O_8, 10 w/o acetylene black, and 40 w/o binder and pressing 1 cm^2 cathode pellets under a pressure of 3 tons/cm^2. Two-electrode cells were assembled by separating a cleaned lithium foil anode and a cathode pellet with a Celgard 2400 porous polypropylene separator soaked with electrolyte. The cells were housed in stainless-steel button cells sealed with polypropylene O-ring sealings.

Three-electrode cells were made as described elsewhere (23) using LiAl reference electrodes and Ni-foil current collectors. An Al strip was wrapped in Celgard 2400 separator soaked with electrolyte, and the anode and cathode were placed on each side of this bag. The cells were clamped between glass plates and inserted into a glass container filled with *ca.* 50 ml electrolyte and closed with a metal lid fitted with an O-ring seal. The α-Al/β-LiAl reference electrode was formed by shorting the lithium counterelectrode and the Al electrode until a stable voltage of about 360 mV *vs.* lithium, corresponding to α-Al/β-LiAl phase equilibrium, was reached.

Lithium was inserted and deinserted by passing a constant current through the cells. The degree of insertion was calculated from the amount of charge passed through the cells. Lithiated samples for x-ray diffraction analysis were prepared by applying a preset, constant voltage to cells kept at 125°C, until the current was stabilized below 1 μA

Table I. Composition and lattice parameters of $Li_xM_yCr_3O_8$. Uncertainty *ca.* 5% on composition. The standard deviations on lattice parameters are given in brackets

Compound	a (Å)	b (Å)	c (Å)	β (°)	Vol. (Å^3)	Preparation
$NaCr_3O_8$	8.492(1)	5.478(2)	6.799(2)	91.44(10)	316.2	Ref. (14)
$Na_{0.8}Cr_3O_8$	8.491(1)	5.475(1)	6.803(1)	91.42(2)	316.2	Pristine mat.
$Li_{0.4}Na_{0.6}Cr_3O_8$	8.494(2)	5.477(1)	6.798(1)	91.40(2)	316.1	n-BuLi, Br_2
$Li_{0.5}Na_{0.8}Cr_3O_8$	8.494(1)	5.476(1)	6.804(1)	91.43(1)	316.4	LiI
$Li_{1.2}Na_{0.7}Cr_3O_8$	8.495(2)	5.474(1)	6.803(1)	91.48(2)	316.3	n-BuLi, I_2
$Li_{2.5}Na_{0.8}Cr_3O_8$	8.499(2)	5.474(1)	6.803(1)	91.44(3)	316.4	n-BuLi
KCr_3O_8	8.569(1)	5.466(1)	7.622(1)	95.25(10)	355.5	Ref. (14)
$K_{0.9}Cr_3O_8$	8.567(1)	5.464(1)	7.622(1)	95.26(2)	355.3	Pristine mat.
$Li_{0.2}K_{1.0}Cr_3O_8$	8.570(2)	5.464(1)	7.621(1)	95.28(1)	355.4	n-BuLi, Br_2
$Li_{0.5}K_{1.0}Cr_3O_8$	8.572(2)	5.461(1)	7.625(1)	95.26(2)	355.4	LiI
$Li_{0.5}K_{0.9}Cr_3O_8$	8.573(3)	5.462(1)	7.619(2)	95.23(3)	355.3	n-BuLi, I_2
$Li_{0.9}K_{1.0}Cr_3O_8$	8.578(2)	5.461(1)	7.623(2)	95.21(2)	355.6	n-BuLi

for at least 12h. The cathodes were dissolved in acetonitrile, and the remaining solids were filtered off, washed repeatedly with acetonitrile, and vacuum dried at *ca.* 60°C. To avoid possible reactions with the atmosphere, some of the samples were coated with kollodium (Merck). However, no difference was observed between x-ray diagrams of materials protected from moisture, etc., and samples exposed to the atmosphere for time periods up to several weeks.

Room-temperature OCV curves of the materials were obtained by passing a known amount of charge through the cells followed by current interruption. The cell potentials were measured after voltage equilibration.

Cyclic voltammetry and ac measurements were conducted on three-electrode cells using a Solartron 1250 frequency response analyzer and a Solartron 1256 electrochemical interface.

Handling of the cell components and cell assemblage, as well as the chemical reactions, took place in either an argon-filled glove box (Braun, <10 ppm H_2O) or in a dry room with relative humidity less than 2%.

Results and Discussion

Electrochemical lithium insertion: $LiCr_3O_8$ constant-current voltage-composition curves obtained at 125°C and at room temperature are shown in Fig. 2a and 3a. At 125°C, three voltage plateaus are observed. At *ca.* 2.9V for $0 < x < 0.65$, at *ca.* 2.25V for $0.65 < x < 2.5$, and at *ca.* 1.8V for $3.5 < x < 5$. Basically, the curves at both temperatures are identical with the exception that the room-temperature voltage (cutoff at 1.0V) is lower than the high-temperature data (cutoff at 1.5V). Continued lithium insertion below 1.5V at 125°C results in a sharp voltage drop to less than 1V *vs.* lithium. The same capacity, *ca.* 5 lithium per formula unit, is obtained at both temperatures. As seen in Fig. 2 and 3, it was only possible to deinsert lithium partly from $Li_xLiCr_3O_8$ at both temperatures, and the second and following lithium insertion curves are different from the initial discharge curves. It was therefore expected that an irreversible structural change of the pristine material is involved in the discharge process. The hump observed at *ca.* $x = 0.3$ during the second discharge at room temperature is also observed at 125°C, but it is not as pronounced as at room temperature. The hump is likewise visible during the following discharges. A possible explanation is a rise of the electronic conductivity consistent with the mixed oxidation states of chromium necessarily present during the insertion and deinsertion processess.

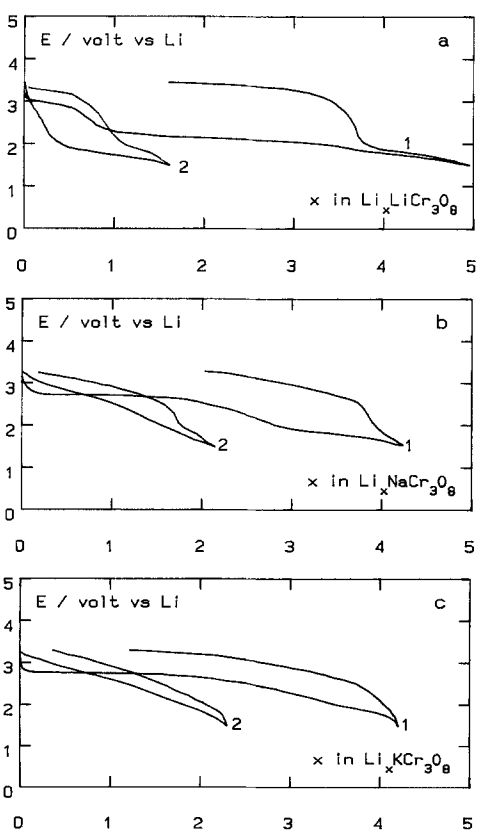

Fig. 2. Voltage-composition curves for constant-current lithium insertion at 125°C in (a) $LiCr_3O_8$ (0.25 mA/cm²), (b) $NaCr_3O_8$ (0.1 mA/cm²), and (c) KCr_3O_8 (0.1 mA/cm²). Cycle numbers are indicated on the figure.

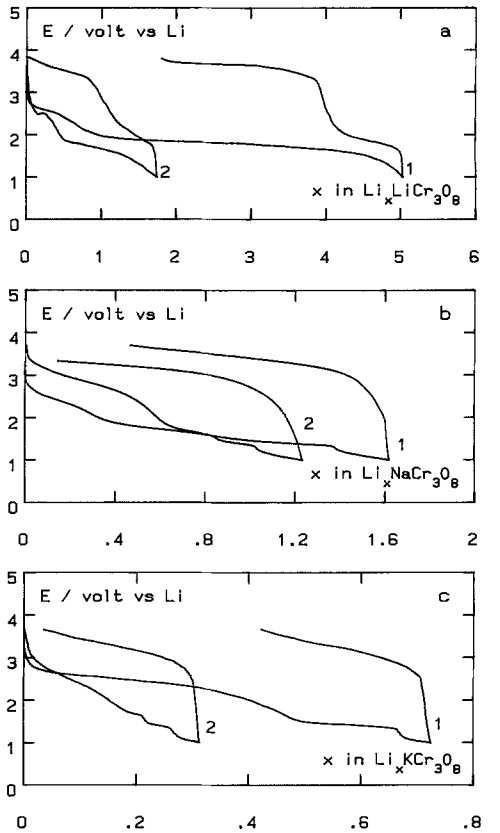

Fig. 3. Room temperature voltage-composition curves for lithium insertion in (a) $LiCr_3O_8$, (b) $NaCr_3O_8$, and (c) KCr_3O_8. Current densities: 0.1 mA/cm². Cycle numbers are indicated on the figure.

The lithium insertion at 125°C in $NaCr_3O_8$ and KCr_3O_8 appears to proceed quite differently from that in $LiCr_3O_8$ (Fig. 2), despite the initial structural similarities. For both $NaCr_3O_8$ and KCr_3O_8 the lithium insertion takes place at a virtually constant voltage, around 2.75V for $x < 2$. For lithium insertion in the range $2 < x < 3$, the voltage curve is sloping while a second plateau develops at $x > 3$. The maximum number of lithium atoms inserted per formula unit exceeds four. Here also, the second and following lithium insertion curves are different from the initial ones, indicating as for $LiCr_3O_8$, that irreversible phase transformation takes place.

X-ray diagrams of $Li_xLiCr_3O_8$, $0 < x < 5$ (potentiostatic lithium insertion at 125°C), confirm that the reaction involves structural breakdown of the pristine material. All the x-ray diagrams show identical diffraction patterns indicating that the structure breaks down upon insertion of small amounts of lithium. Similar analysis of KCr_3O_8 shows that the structure is retained during electrochemical insertion of at least 2.5 lithium atoms per formula unit at 125°C. Continued lithiation of $Li_xKCr_3O_8$ ($x > 4$) apparently leads to more severe structural changes in accordance with the change in oxygen coordination around chromium by reduction of Cr(IV) to Cr(III). Due to the poor quality of the x-ray diagrams (line broadening), it was impossible to calculate and refine unit cell parameters of the preserved phases and a proper identification of the reaction products of the displacement reactions was not possible either (15).

At room temperature, the effects of the structural differences between $NaCr_3O_8/KCr_3O_8$ and $LiCr_3O_8$ are more pronounced than at 125°C (Fig. 3). Less than one lithium is accepted by KCr_3O_8 above 1V *vs.* lithium. After a sharp initial voltage drop, the voltage decreases gradually from *ca.*

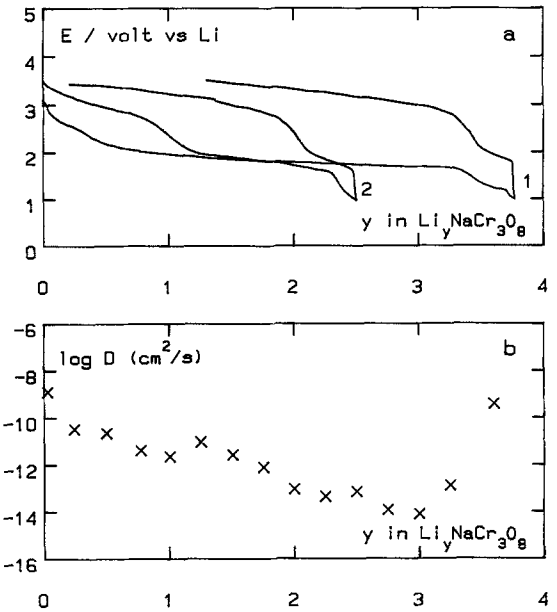

Fig. 4. Room temperature (a) OCV curves of Li/$NaCr_3O_8$ and (b) compositional dependence of D_{Li}.

2.75V to *ca.* 1.60V ($x = 0.45$) after which the voltage is fairly constant until *ca.* $x = 0.65$, where the voltage drops abruptly by 200-300 mV. The shape of the $NaCr_3O_8$ discharge curve seems to be a combination of the $LiCr_3O_8$ curve at high voltage and that of KCr_3O_8 at lower voltage (below 1.7V). However, the shapes of the second and following discharge curves of $NaCr_3O_8$ and KCr_3O_8 are similar, even though the initial capacity of the former lies between that of $LiCr_3O_8$ and KCr_3O_8.

The OCV curves of Li/$NaCr_3O_8$ and Li/KCr_3O_8 cells obtained by intermittent constant-current lithium insertion and deinsertion at room temperature are shown in Fig. 4 and 5, respectively. The $NaCr_3O_8$ OCV curve has essentially the same shape as the corresponding constant-current curve. However, the number of Li atoms inserted is close to four. The OCV curve for KCr_3O_8 is sloping and nearly featureless for $x < 1$, while two small plateaus are seen at *ca.* 1.65 and 1.2V. Approximately 1.3 Li atoms are inserted per formula unit.

As pointed out by Besenhard *et al.* (7), lithium ion diffusion coefficients determined on polycrystalline materials in porous cathodes should be understood as apparent values rather than material constants because of the uncertainties involved in the determination of, *e.g.*, effective surface area, particle size, and orientation effects. It therefore appears to be of interest to investigate the compositional dependence of the apparent diffusion coefficient. Lithium diffusion coefficients were determined by the galvanostatic intermittent titration technique described by Weppner and Huggins (24) using the equation

$$D_{Li} = 4/\pi \cdot (V_m \cdot I_o/S \cdot \mathbf{F} \cdot z)^2 \cdot \{(dE/dx)/[dE/d(\sqrt{t})]\}^2$$

where D_{Li} is the lithium diffusion coefficient (cm^2/s), V_m the molar volume (cm^3/mole), I_o the current (A), S the contact area of the sample-electrolyte interface (cm^2), z is the valence of Li^+, $\mathbf{F}$ is the Faraday constant, dE/dx is the slope of the OCV curve, and $dE/d(\sqrt{t})$ is the slope of the E *vs.* square root t curve. The area was taken as the geometrical area of the porous cathodes used. Lithium diffusion coefficients were determined for lithium insertion in both $NaCr_3O_8$ and KCr_3O_8 (Fig. 4 and 5) as a function of the degree of insertion. During lithium insertion in $NaCr_3O_8$, D_{Li} decreases linearly by several orders of magnitude in the insertion range $0 < x < 3$. For $x > 3$, D_{Li} increases abruptly to near the initial value. Similar trends are observed for lithium insertion in KCr_3O_8, although the degree of insertion does not exceed 1.3 Li/KCr_3O_8. Also, the diffusion coefficients have similar values in the insertion range $0 < x < 1.3$ (10^{-9}-10^{-12} cm^2/s). Thus, the lower degree of lithium insertion in KCr_3O_8 compared to $NaCr_3O_8$ is not caused by a slower lithium diffusion process. This is surprising in view of the structural and chemical similarities between these two compounds, but is possibly explained by either the larger channel diameters of KCr_3O_8, causing a pinning of the lithium ions at the channel walls thereby blocking the channels for further lithium insertion, or by the larger size of the potassium ion, 1.55Å, as compared to 1.24Å for the sodium ion (25). Due to the larger size, the potassium ion might block the diffusion paths for lithium ion movement.

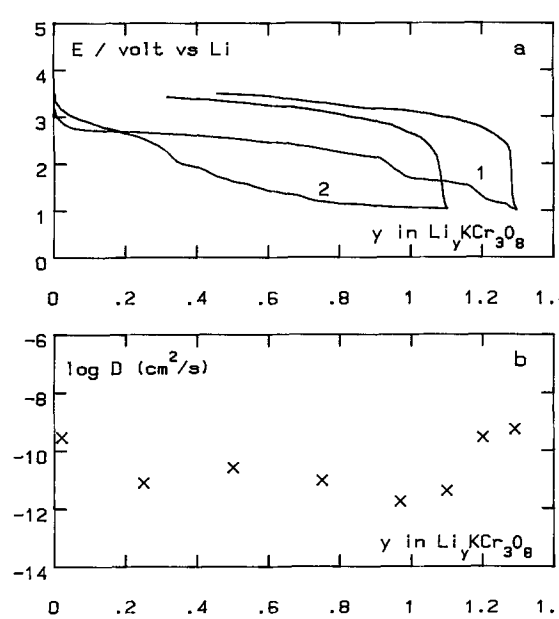

Fig. 5. Room temperature (a) OCV curves of Li/KCr_3O_8 and (b) compositional dependence of D_{Li}.

The reversibility of the reactions is limited by the ability to remove the inserted lithium ions as seen by repeated lithium insertion at both 125°C and room temperature. The capacity leveled off at $x < 1$ in $Li_xMCr_3O_8$ for all the compounds at room temperature, and also $LiCr_3O_8$ at 125°C. In $NaCr_3O_8$, more than three lithium atoms per formula unit could be repeatedly inserted above 3.7V at 125°C (15), although the polymer electrolyte used is electrochemically unstable above 3.5V at this temperature (26).

The average oxidation state of +5 of chromium in MCr_3O_8 allows the possibility of deinsertion of the alkali metal ion and simultaneous oxidation of the chromium to a higher average oxidation state. As mentioned in the introduction, it is possible to oxidize Cr(III) to Cr(IV) without introducing major structural changes, as is demonstrated in $LiCrO_2$ and $NaCrO_2$. The deinsertion of alkali metal ions from MCr_3O_8 was investigated by cyclic voltammetry in oxidation of freshly prepared cells. At a scan rate of 0.5 mV/s, no appreciable cathodic current was observed up to 4V *vs.* lithium. It therefore appears that the alkali metal ions in the pristine materials are immobile.

AC spectroscopy.—The behavior of the three chromium oxide composite cathodes was characterized upon electrochemical lithium insertion by ac spectroscopy at room temperature. The results obtained for these three cathodes were coherently analyzed according to the model proposed by Thomas *et al.* (27) which involves the formation of a surface layer at the cathode-electrolyte interface, through which ions have to migrate before charge transfer can occur.

All three chromium oxide cathodes show similar ac spectra composed of two series-connected convoluted RC equivalent components. In Fig. 6, complex plane impedance spectra obtained with $LiCr_3O_8$ as a function of voltage are presented. The first RC component, at higher frequency, was in this case invariant between 3.0 and 1.2V. It is believed that this RC component is related to the surface layer (R_{sl} 25 Ω/cm^2, C_{sl} 0.6 μF/cm^2, τ_{sl} $1.6 \cdot 10^{-5}$ s). The second component of the spectrum had a larger resistance at 3V (R_{ct} = 500 Ω/cm^2) which decreased markedly upon insertion of small amounts of lithium, down to R_{ct} = 65 Ω/cm^2, then remaining constant until $x = 4.5$ (Fig. 7a). For

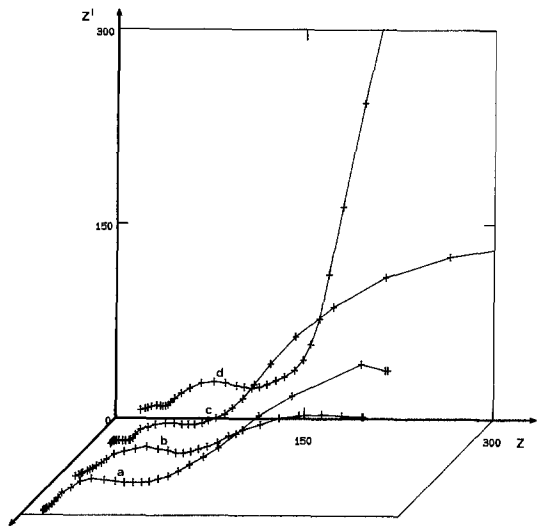

Fig. 6. Room-temperature complex plane ac impedance spectra of $Li_{1+x}Cr_3O_8$-based composite cathode at the following potentials, (a) 2.1V, (b) 1.9V, (c) 1.6V, and (d) 1.3V in the frequency range 65-0.1 Hz and an amplitude of 25 mV. The units of Z and Z' are ohm.

insertion levels higher than $x = 4.5$, the value of R_{ct} goes through a minimum followed by an increase. These latter variations of R_{ct} occur in the insertion range where Cr(IV) is reduced to Cr(III). The variation of the capacitive terms and of the relaxation times as a function of the insertion level are shown in Fig. 7b. They indicate, as does the variation of the resistive terms, that changes occur mainly after insertion of small amounts of lithium ($x << 1$) and when Cr(IV) is reduced to Cr(III).

In the case of $NaCr_3O_8$, a similar general behavior was observed even if smaller amounts of lithium could be inserted. In Fig. 8, we report the variations of the RC parameters of the ac spectra, as a function of the insertion level. For this system components the R_{sl} and C_{sl} vary for $x < 1$, then remain almost constant for $1 < x < 4$. Since τ_{sl} was constant for all values of x, the observed variations of R_{sl} and C_{sl} could be attributed to geometrical variations of the active cathode. However, x-ray results indicated no phase change and only minor volume changes of the unit cell (see later). Also, values of R_{sl}, C_{sl}, and τ_{sl} are all greater than those calculated for the $LiCr_3O_8$ cathode. This result indicates that the nature of the surface layer is different in the two systems.

The values of R_{ct}, after an initial increase for $x < 0.5$, decrease continuously until $x = 4$, which could also indicate an increase of the active surface area. This is not confirmed by the variation of C_{ct}, which remains almost constant at *ca.* 800-1000 $\mu F/cm^2$ over the active range of x. This value of C_{ct} is much larger than the one calculated for $LiCr_3O_8$.

The results obtained with KCr_3O_8 are closely related to those for $NaCr_3O_8$. Thus, the $LiCr_3O_8$, $NaCr_3O_8$-, and KCr_3O_8-based cathodes all showed the formation of a surface layer for which the composition and rate-determining step is different for the $LiCr_3O_8$ compared to the Na and K chromium oxides. The active surface areas for charge transfer are larger for the (Na, K)Cr_3O_8 (based on C_{dl}) than for $LiCr_3O_8$, even if structural breakdown was observed only for $LiCr_3O_8$. These results indicate that the mechanism by which lithium is electrochemically inserted in the chromium oxides can differ markedly, and that the achieved level of insertion depends more on the intragranular diffusion coefficient than on R_{ct}.

Chemical lithium insertion.—All three compounds retain their black color, independent of the extent of insertion. The composition and refined lattice parameters for $NaCr_3O_8$, KCr_3O_8, and the corresponding lithiated compounds are given in Table I. The composition of the lithium form of MCr_3O_8 was $Li_{1.2}Cr_3O_8$. Contrary to the behavior of $NaCr_3O_8$ and KCr_3O_8, lithiation of $LiCr_3O_8$ leads to structural breakdown.

Reaction with LiI.—LiI is a mild lithiation reagent. The reaction corresponds to *ca.* 2.8V *vs.* lithium (22), which again by comparison with the discharge curves (Fig. 3-5) corresponds to less than 0.5 Li/MCr_3O_8 inserted electrochemically. As is seen in Table I, the number of lithium atoms inserted chemically in $NaCr_3O_8$ and KCr_3O_8 per formula unit is *ca.* 0.5. In $LiCr_3O_8$, 0.6 lithium atom was inserted per formula unit.

Reaction with n-BuLi.—Reaction with n-BuLi corresponds to 1.0V *vs.* lithium (22). By reacting $LiCr_3O_8$, $NaCr_3O_8$, and KCr_3O_8 with n-BuLi, the same trend is observed as during electrochemical lithium insertion; *ca.* four lithium atoms per formula unit are inserted in $LiCr_3O_8$ and less than one in KCr_3O_8. The amount of lithium accepted by $NaCr_3O_8$ lies between that of $LiCr_3O_8$ and KCr_3O_8.

Delithiation with I_2.—Contrary to n-BuLi, the I_2/I^- system is reversible (22). Thus, lithium extraction with I_2 of the highly lithiated compounds $Li_xMCr_3O_8$, should result in the same stoichiometry as lithiation of the pristine materials with LiI, provided the reaction is reversible. The data

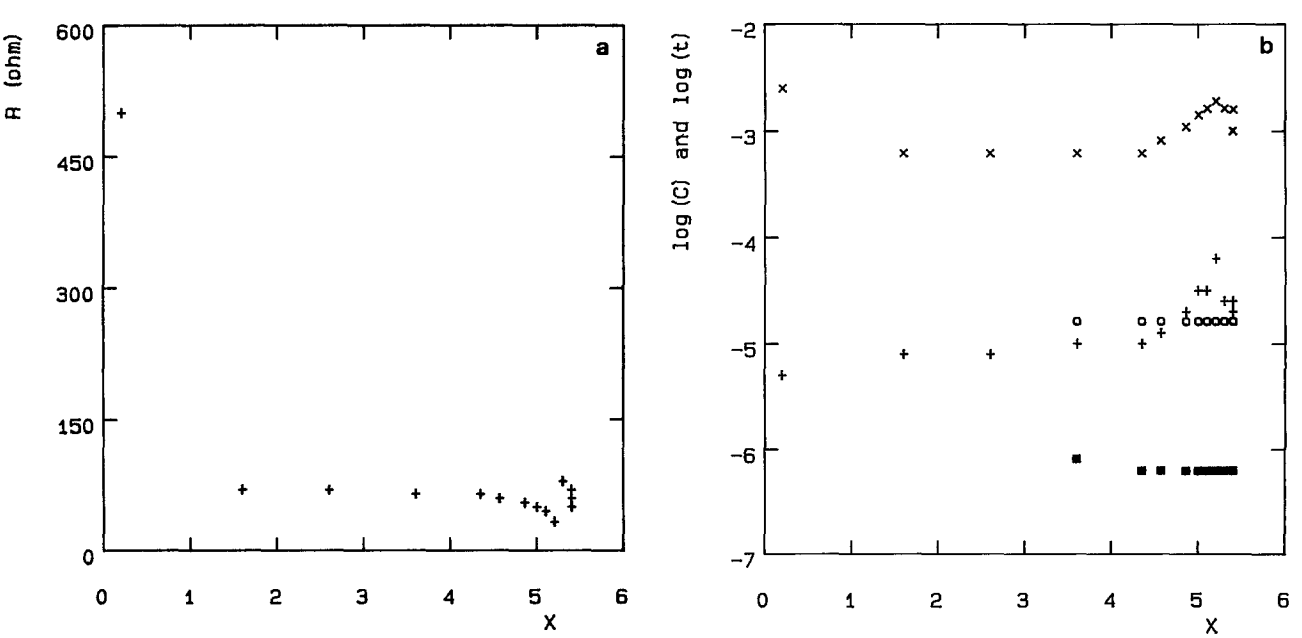

Fig. 7. (a, left) Variation of R_{ct} and (b, right) variation of (■) log(C_{sl}), (○) log(τ_{sl}), (+) log(C_{dl}), and (×) log(τ_{dl}) as functions of insertion level (×) in $Li_{1+x}Cr_3O_8$ at room temperature.

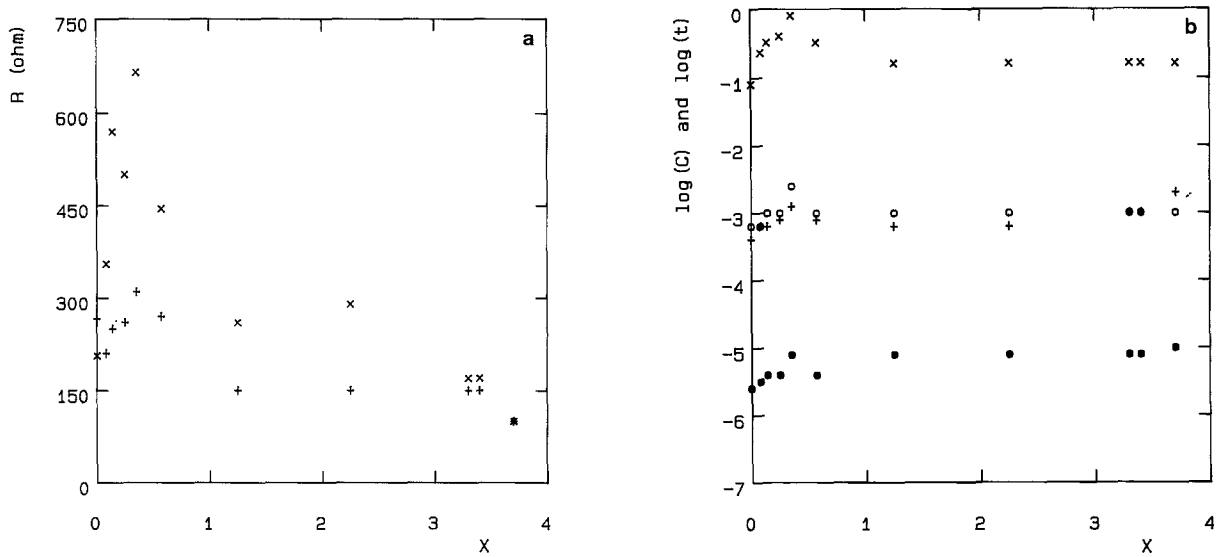

Fig. 8. (a) Variation of (+) R_{sl} and (×) R_{ct} and (b) variation of (●) log(C_{sl}), (○) log(τ_{sl}), (+) log(C_{dl}), and (×) log(τ_{dl}) as a function of lithium insertion (×) in $Li_xNaCr_3O_8$ at room temperature.

in Table I show that this is indeed the case for the Li/KCr_3O_8 system, the same number of Li/KCr_3O_8 are present in the two compounds. For both $LiCr_3O_8$ and $NaCr_3O_8$, more than twice the amount of lithium is present in the compounds (3.7 Li/$LiCr_3O_8$ and 1.2 Li/$NaCr_3O_8$) after treatment with n-BuLi and I_2 than after treatment with LiI.

Delithiation with Br_2.—Chemical delithiation with Br_2 corresponds to electrochemical charging to *ca.* 3.5V (22) *vs.* lithium, and bromine is therefore capable of deinserting more lithium than iodine. Furthermore, the bromine potential *vs.* lithium is higher than the OCVs of the pristine materials (3.1-3.2V *vs.* Li). It is expected that bromine deinserts at least the amounts of lithium inserted, but it also deinserts part of the alkaline metals present in the pristine materials, provided they are mobile. However, lithium is still present in all three compounds after deinsertion with bromine (Table I and 0.9 Li/$LiCr_3O_8$) and decreasing in the order $LiCr_3O_8 > NaCr_3O_8 > KCr_3O_8$. The potassium content is practically unchanged in all the experiments while the sodium content is decreasing, probably due to ion exchange with lithium.

X-ray diffraction experiments reveal that the structures of $NaCr_3O_8$ and KCr_3O_8 are preserved during both lithiation and delithiation. The x-ray diagrams were indexed in the same space group as the pristine materials (C2/m) and unit cell parameters were refined using program CELLKANT (31). Contrary to the expectation that lithium insertion leads to an increased layer distance (expansion parallel to the c-axis), the data indicate a small increase of the a-axis, *i.e.*, within and parallel to the $(Cr_3O_8^-)_n$ layers (Table I). The variations of the b and c unit cell axes are insignificant, as are the volume changes of the unit cells.

IR spectroscopy.—For $LiCr_3O_8$, both electrochemical data and x-ray analysis show that the structure breaks down during lithium insertion. However, for $NaCr_3O_8$ and KCr_3O_8 the electrochemical data indicate irreversible structural changes upon cycling, while x-ray analysis shows that the structures of the pristine materials are preserved. Further characterization of the lithium insertion in these two compounds was therefore necessary.

The Cr(VI)—O bonds are considerably shorter than the Cr(III)—O bonds, and therefore have higher stretching frequencies. The main absorption bands of Cr(III)—O occur at 640 and 580 cm^{-1}, while absorption bands at *ca.* 900 cm^{-1} are associated with Cr(VI)—O groups in a variety of chromates. However, in dichromates additional peaks are present between 700 and 800 cm^{-1} (28, 29). Cr(V)—O stretching frequencies are reported to appear at *ca.* 815 cm^{-1}, as in, *e.g.*, Li_3CrO_4 (30). Therefore, a gradual lowering of the chromium-oxygen vibrational stretching frequencies is expected when Cr(VI) is progressively reduced to chromium in lower oxidation states by lithium insertion. Accordingly, the variations of the stretching frequencies were followed by IR spectroscopy.

$NaCr_3O_8$ and KCr_3O_8 contain one Cr—O bond which is considerably shorter than all the other Cr—O bonds. For KCr_3O_8, this bond length is 1.53Å as compared to 1.65Å for the remaining tetrahedral Cr—O bonds and *ca.* 1.95Å for the octahedral Cr—O bonds. The oxygens of the latter groups are shared between octahedra and tetrahedra and give rise to the absorption bands at *ca.* 800 cm^{-1} as well as the overall complexities of the spectra. The short Cr—O bond is correlated to one CrO_4 tetrahedra only and can be considered to be a Cr=O double bond associated with the absorption bands at *ca.* 900 cm^{-1} (28).

The IR spectra, in the region 300-1200 cm^{-1}, of $NaCr_3O_8$ and KCr_3O_8 as well as of the chemically lithiated and delithiated compounds, are shown in Fig. 9. At frequencies above 1200 cm^{-1}, all spectra are essentially featureless. The spectra of $LiCr_3O_8$ (not shown) and KCr_3O_8 agree well with the spectra reported by Foster and Hambly (20).

Insertion of 0.9 Li/MCr_3O_8 in KCr_3O_8 causes a shift of the high-frequency absorption at 902-894 cm^{-1}. Furthermore, an absorption shoulder appears at *ca.* 700 cm^{-1}. The variation in bonding character induced by treatment with LiI,

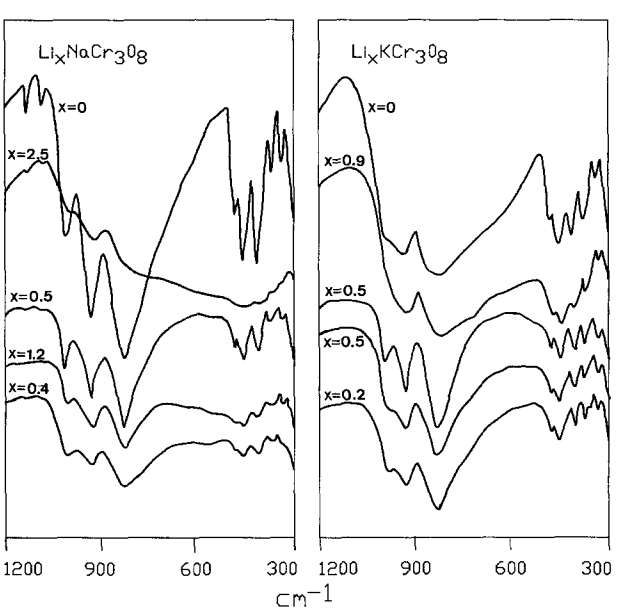

Fig. 9. IR transmission spectra of $NaCrCr_3O_8$ and KCr_3O_8 compared to chemically lithiated and delithiated compounds. From top: pristine material, reaction with *n*-BuLi, LiI, *n*-BuLi/I_2, and *n*-BuLi/Br_2. The compositions are indicated in the figure.

as well as lithium deinsertion with I_2 and Br_2, are too small to be detected in this case.

The stretching frequency of the Cr=O double bond of $NaCr_3O_8$ decreases from 896 to 880 cm^{-1} by reaction with n-BuLi. The overall features of the spectrum of the original material are still visible, although a broad absorption band appears in the range 750-500 cm^{-1}. A similar treatment of $LiCr_3O_8$ (not shown) results in a broad absorption band with a maximum at *ca.* 500 cm^{-1} consistent with almost complete reduction of Cr(VI) to Cr(III). Delithiation of $NaCr_3O_8$ and KCr_3O_8 leads to an increase of the stretching frequencies to the values observed for the pristine materials.

Apparently, chromium is present in mixed oxidation states between Cr(VI) and Cr(III) in both $NaCr_3O_8$ and KCr_3O_8 during lithium insertion, and the oxygen coordination around chromium is essentially preserved.

Thermal stability.—The DSC traces of $NaCr_3O_8$ and KCr_3O_8 and the corresponding n-BuLi—treated compounds are shown in Fig. 10. The compounds were examined in the temperature range −30°-600°C. As no reactions were observed at lower temperatures, only the range 300°-600°C is shown.

The most remarkable feature is that the lithiated compounds appear to be as thermally stable as the pristine materials.

For both KCr_3O_8 and $NaCr_3O_8$, only one endothermic reaction is observed, at 453° and 456°C, respectively. The thermal behavior of the lithiated compounds deviates both from each other and from those of the pristine materials. By heating of $Li_{2.5}NaCr_3O_8$, an exothermic reaction at 369°C precedes an endothermic reaction at 419°C. Heating of $Li_{0.9}KCr_3O_8$ shows an exothermic reaction at 391°C, followed by two endothermic reactions at 393° and 422°C, respectively. In addition, a broad exotherm is observed at 501°C.

X-ray analysis of samples heated to 600°C revealed the presence of Cr_2O_3 as the major constituent of the decomposition products of both $Li_{2.5}NaCr_3O_8$ and $Li_{0.9}KCr_3O_8$. No dichromates were observed, consistent with the decomposition of the lithium, sodium, and potassium dichromates at temperatures below 600°C. Contrary to $Li_2Cr_2O_7$ and $Na_2Cr_2O_7$, which decompose at temperatures around 400°C, $K_2Cr_2O_7$ decomposes at 500°C and the DSC peak observed at 501°C for $Li_{0.9}KCr_3O_8$ may thus be associated with this reaction. A proper identification of the compounds besides Cr_2O_3 from the x-ray diagrams was not possible. These compounds are probably chromates of the types $(Li, Na)_2CrO_4$ and $(Li, K)_2CrO_4$.

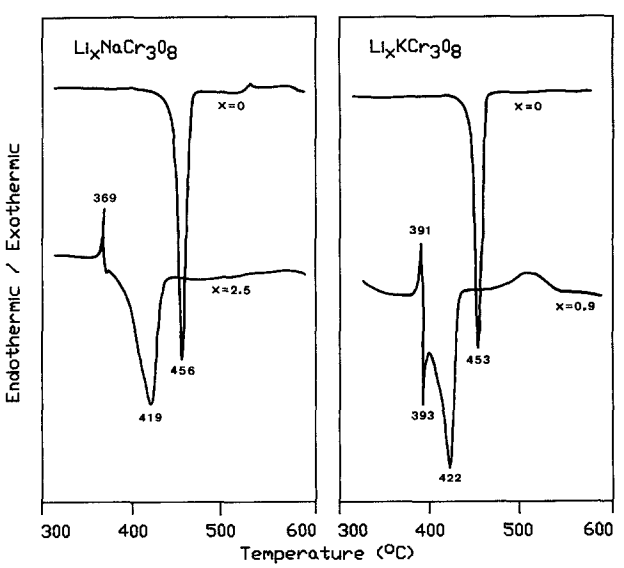

Fig. 10. Comparison of DSC traces of $Li_xMCr_3O_8$ (M = Na, K) and the pristine materials. The materials were contained in closed Pt-ampuls and the heating rate was 10°C/min. The peak temperatures are indicated in the figure.

Conclusion

At temperatures above 100°C, all three materials are able to accommodate more than four lithium atoms per formula unit. At room temperature, however, both chemical and electrochemical evidence shows that the amount of lithium inserted decreases with increasing size of the alkali metal ion present in the pristine materials. The experimental data also show different lithium insertion reactions.

As at elevated temperatures, $LiCr_3O_8$ takes up *ca.* five lithium atoms per formula unit at room temperature, but the pristine material is prone to irreversible structural breakdown during lithium insertion at both temperatures, and the reactions seem to be identical. The structural breakdown already takes place upon insertion of small amounts of lithium, and the reaction is irreversible. Lithium insertion in $NaCr_3O_8$ and KCr_3O_8 at both temperatures proceeds quite differently from that in $LiCr_3O_8$. At a current density of 0.1 mA/cm^2, less than two and one Li/MCr_3O_8 are inserted, respectively, at room temperature. Complete reduction of all Cr(VI) to Cr(III) demands six Li/MCr_3O_8. However, the insertion of more than four Li/MCr_3O_8 involves reduction of Cr(IV) to Cr(III), and a change of oxygen coordination around chromium is therefore to be expected.

A detailed structural knowledge regarding the sites occupied by lithium in the lithiated $NaCr_3O_8$ and KCr_3O_8 is lacking. Although the shape of the discharge curves indicates structural changes, x-ray, IR, and DSC analyses of chemically lithiated compounds show that the structure is preserved during lithium insertion.

By galvanostatic intermittent current lithium insertion at room temperature, close to four lithium atoms are inserted in $NaCr_3O_8$ while only *ca.* 1.3 lithium is inserted in KCr_3O_8. This difference is surprising since the two compounds are isostructural and x-ray analysis of chemically lithiated and delithiated $NaCr_3O_8$ and KCr_3O_8 show no structural changes. The difference in unit cell volumes between pristine $NaCr_3O_8$, KCr_3O_8, and the fully lithiated $NaCr_3O_8$ and KCr_3O_8 are negligible, though some correlation between the lithium content and the length of the a-axis was observed. Only the difference in size between the two interlayer alkali metal ions can be responsible, *i.e.*, the structure containing potassium has two large channel diameters in which the lithium is pinned to the walls or potassium blocks the lithium ion diffusion paths. The low lithium ion diffusion coefficients prevent applications as cathode materials in lithium batteries operating at room temperature. Even at elevated temperatures, electrochemical lithium deinsertion appears to be difficult because some of the lithium ions are tightly bound and are removed only at potentials above 3.7V. The specific energy of $LiCr_3O_8$, calculated for the first room temperature discharge to 1V *vs.* lithium, is 690 Wh/kg. This compound is therefore of interest as an active cathode material in primary lithium batteries.

Thermally, the fully lithiated compounds seem to be as stable as the pristine materials. It appears therefore to be possible to prepare stable chromium oxide containing chromium in mixed oxidation states between Cr(VI) and Cr(III).

Acknowledgment

The authors wish to thank S. Yde-Andersen, H&L Engineering, J. Engell, and The Technical University of Denmark for helpful discussions.

Manuscript submitted June 20, 1988; revised manuscript received Aug. 18, 1988.

H&L Engineering assisted in meeting the publication costs of this article.

REFERENCES

1. B. L. Chamberland, M. P. Herrero-Fernandez, and T. A. Hewston, *J. Solid State Chem.*, **59**, 111 (1985).
2. A. F. Wells, "Structural Inorganic Chemistry," 5th ed., p. 1197, Clarendon Press, Oxford (1984).
3. K.-A. Wilhelmi, Univ. Stockholm, Inorg. Chem., 1966, Dis no. 21.
4. S. Miyazaki, S. Kikkawa, and M. Koizumi, *Synth. Met.*,

6, 211 (1983).
5. J. O. Besenhard and R. Schollhorn, *This Journal,* **124,** 968 (1977).
6. J. O. Besenhard, J. Heydecke, and H. P. Fritz, *Solid State Ionics,* **6,** 215 (1982).
7. J. O. Besenhard, J. Heydecke, E. Wudy, and H. P. Fritz, *ibid.,* **8,** 61 (1983).
8. Y. Takeda, R. Kanno, Y. Tsuji, O. Yamamoto, and H. Taguch, *J. Power Sources,* **9,** 325 (1983).
9. Y. Takeda, R. Kanno, Y. Tsuji, and O. Yamamoto, *This Journal,* **131,** 2006 (1984).
10. Y. Takeda, R. Kanno, Y. Oyabe, and O. Yamamoto, *J. Power Sources,* **14,** 215 (1985).
11. T. A. Hewston and B. L. Chamberland, *J. Magn. Magn. Mat.,* **43,** 89 (1984).
12. K.-A. Wilhelmi, *Ark. Kemi,* **26,** 131 (1966).
13. K.-A. Wilhelmi, *Acta Chem. Scand.,* **12,** 1965 (1958).
14. K.-A. Wilhelmi, *Chem. Commun.,* 437 (1966).
15. R. Koksbang, S. Yde-Andersen, K. West, R. Zachau-Christiansen, and S. Skaarup, *Solid State Ionics,* **28-30,** 868 (1988).
16. W. Klemm, *Z. Anorg. Allg. Chem.,* **301,** 323 (1959).
17. T. Tsutsumi, I. Ikemoto, T. Namikawa, and H. Kuroda, *Bull. Chem. Soc. Jpn.,* **54,** 913 (1981).
18. L. Suchow, I. Fankuchen, and R. Ward, *J. Am. Chem. Soc.,* **74,** 1678 (1952).
19. K.-A. Wilhelmi, *Acta Chem. Scand.,* **22,** 2565 (1968).
20. J. J. Foster and A. N. Hambly, *Aust. J. Chem.,* **29,** 2137 (1976).
21. M. Armand, in "Fast Ion Transport in Solids" W. van Gool, Editor, pp. 665-673, North-Holland Publishing Company, Amsterdam (1973).
22. D. W. Murphy, *Proc. Electrochem. Soc.,* **7,** 197 (1980).
23. D. Fauteux, Ph.D. Thesis, INRS-Energie, Varennes, Que., Canada (1986).
24. W. Weppner and R. A. Huggins, *This Journal,* **117,** 1569 (1977).
25. R. D. Shannon, *Acta Crystallogr., Sect. A,* **32,** 751 (1976).
26. M. B. Armand, *Solid State Ionics,* **9/10,** 745 (1983).
27. M. G. S. R. Thomas, P. G. Bruce, and J. B. Goodenough, *This Journal,* **132,** 1521 (1985).
28. C. G. Barraclough, J. Lewis, and R. S. Nyholm, *J. Chem. Soc.,* 3552 (1959).
29. J. A. Campbell, *Spectrochim. Acta,* **21,** 1333 (1965).
30. J. E. Guerchais, M. J. Leroy, and R. Rohmer, *C. R. Acad. Sci., Paris,* **261** 3628 (1965).
31. N. O. Ersson, program CELLKANT, Chemical Institute, Uppsala University, Uppsala, Sweden (1981).

Degradation Mechanisms of Nylon Separator Materials for a Nickel-Cadmium Cell in KOH Electrolytes

H. S. Lim,* J. D. Margerum,* S. A. Verzwyvelt,* A. M. Lackner, and R. C. Knechtli

Hughes Research Laboratories, Malibu, California 90265

ABSTRACT

Degradation reactions of a nylon 6 battery separator material have been studied in 4-34% aqueous KOH electrolytes at 35°-110°C. In a Ni/Cd cell, this degradation involves a slow hydrolysis reaction followed by fast electrochemical oxidations of the hydrolysis reaction products. Arrhenius activation energy of the hydrolysis reaction in 34% KOH was 20.0 ± 0.3 kcal/mole. A plot of the hydrolysis rate at 100°C *vs.* hydroxyl ion concentration gave a rate maximum at about 16% KOH, and the mechanism for this effect is discussed. Electrochemical oxidations of the hydrolysis product, 6-aminocaproate ion, appear to proceed rapidly in several sequential steps at a nickel oxide electrode. In a Ni/Cd cell, the combination of nylon separator hydrolysis followed by electrochemical oxidation of the products can seriously degrade the battery lifetime. The rate of the hydrolysis of nylon 66 separator material was approximately one half of that of the nylon 6 material.

A nonwoven nylon felt (Pellon 2505[1] which is made of nylon 6) has been used as a standard separator material in aerospace Ni/Cd battery cells. Until recently, this battery has been used almost exclusively as the energy storage device for long life spacecraft such as communication satellites. The lifetime of these batteries was previously one of the life limiting factors of the spacecraft, particularly due to the degradation of the nylon separator material as we had reported earlier (1). Although the problem of nylon degradation was recognized previously (2), there has been relatively little quantitative work published on the mechanism and rate of the degradation. Our preliminary study showed that the chemical and electrochemical degradation of nylon can cause lifetime problems for the Ni/Cd cell. Therefore, it is important for the battery industry to understand the degradation rate and mechanism of the nylon materials in Ni/Cd cells. Although for some high-power satellites (approximately 2 kW or higher) the battery is being replaced by newly developed Ni/H_2 batteries, the Ni/Cd battery is expected to remain as the workhorse for smaller power satellites. Ni/Cd cells with alternate nylon material (Pellon 2536) are recently being developed (as the Pellon 2505 became unavailable commercially). In other cell designs, nylon separators are replaced with a zirconia separator (3-7).

Nylon is well known to hydrolyze rapidly in acids but is relatively stable toward hydrolysis in bases (8). It is also known to degrade in neutral media by air oxidation (9). However, limited information was available on the base hydrolysis of nylon 6 of which the separator material is made. A close monomeric structure to this nylon may be ϵ-caprolactam which has an analogous peptide bonding to the nylon. The ϵ-caprolactam was reported (10) to follow the first-order kinetics of a chemical reaction with respect to its concentration and first-order in hydroxyl ion concentration. The present report describes results of our accelerated studies on the nylon felt hydrolysis as a function of temperature and KOH concentration and the electrochemical oxidations of the nylon hydrolysis product at a nickel oxide electrode, and also includes a discussion of a possible mechanism of the hydrolysis. The hydrolysis rates of a nylon 66 felt material are compared with those of nylon-6 felt. Activation energy of the hydrolysis rates has been determined. Nylon degradation rates at an operation temperature of a Ni/Cd cell can be estimated using this activation energy and elevated temperature data.

Experimental

Reagents.—Potassium hydroxide used in the study was Baker analyzed reagent grade. Acetonitrile (AN) was "distilled in glass" grade by Burdick and Jackson Laboratories, Incorporated. Bis-(trimethylsilyl)acetamide (BSA) was a specially purified grade by Pierce Chemical Company. Bis-2-(2-methoxyethoxy)ethyl ether (BMEE) purchased from MC/B Chemical was purified before use by a fractional distillation after refluxing with sodium to react with any trace peroxide. Triethylamine (TEA) was used as purchased from Aldrich Chemical Company. Reagent-

*Electrochemical Society Active Member.

[1] This Pellon 2505 (zinc chloride-bonded) is no longer manufactured. Its popular replacement is Pellon 2536 (hot inert gas bonded) which is made of a mixture of nylon 6 and nylon 66.